www.czasopisma.pan.pl PAN www.journals.pan.pl

ARCHIVES of FOUNDRY ENGINEERING

ISSN (2299-2944)
Volume 2021
Issue 4/2021

61 – 66

10.24425/afe.2021.138680

8/4

Published quarterly as the organ of the Foundry Commission of the Polish Academy of Sciences

Analysis of Proportional Scopes on Probability Density Functions of Random Chords of Spherical Particles

D. Gurgul
AGH University of Science and Technology, Kraków, Poland
Corresponding author. E-mail address: dg@agh.edu.pl

Received 17.09.2021; accepted in revised form 04.11.2021

Abstract

The paper presents an experimental confirmation of the fact that if a three-dimensional volume does not contain spherical particles with particular size, the Probability Density Function (PDF_1) of half-chord lengths has proportional ranges. This fact has been deduced in work [1] during the derivation process of the Probability Density Function (PDF_3) that maps the particle radii on the basis of data (PDF_1) collected from flat cross-sections. The experiment has been executed virtually by using a simple computer program written in the C++11 language. The computer generation of particles allowed imposing various kinds of known PDF_3 and the ranges in which the particles could not be created. Next, the virtual nodules have been used to produce sets of chords that served as input data to create histograms that approximated the continuous PDF_1. Having such histograms, it was possible to reveal proportional scopes of the PDF_1. The proportional dependencies occurred in the same ranges where the nodules had not been generated.

Keywords: Probability density function of random chords distribution, Linear analysis, Particle size distribution

1. Introduction

One of the stereological tasks is the mapping of a volumetric size distribution of spherical particles in non-transparent materials on the basis of data collected from flat cross-sections. Methods that use the data obtained from the cross-sections are usually categorized into three groups. The first group uses, as input data, mark radii or diameters of cuts of spherical particles [2-4]. Into the second group, methods that use areas of marks of intersected nodules can be included [5]. The last group includes solutions that employ random chords from a metallographic analysis [6-8]. The thing which is common among the aforementioned methods is the fact that all of them try to reflect the size distribution of three-dimensional particles, randomly placed in a volume, having only data received from flat cross-sections. The data obtained from metallographic specimens serve as a source to build various histograms that represent mark radii, areas of marks, and chord lengths. In turn, these histograms are used in equations that approximate the real and unknown form of the Probability Density Function of the particle radii (PDF_3).

In paper [1] a formula that maps PDF_3 on the basis of PDF_1 describing half-chord size distributions has been derived. The form of the equation is the following:

$$f_3(x) = \frac{\overline{S}}{2\pi}\left(\frac{f_1(x)}{x^2} - \frac{1}{x}\frac{\mathrm{d}\, f_1(x)}{\mathrm{d}x}\right) \tag{1}$$

where:

$f_3(x)$ – probability density function of the particle radii (PDF_3),
$\overline{S}$ – external mean area of the nodules,

$f_1(x)$ – probability density function of the half-chord lengths (PDF_1).

It should be emphasised that both functions $f_1(x)$ and $f_3(x)$ in Eq. (1) are continuous, whereas in practice, we can only approximate them by histograms built from discrete values obtained from metallographic measurements. During the derivation of the function $f_3(x)$ it has been shown in [1] that if any range of the $f_1(x)$ has a proportional dependency, the function $F_3(x)$ must be constant in this region and as a consequence $f_3(x)$ equals zero:

$$f_1(x) = \frac{8\pi x}{\overline{S}}\left(1 - F_3(x)\right) \tag{2}$$

where:

$F_3(x)$ – cumulative distribution function of the particle radii (CDF_3).

The zero value of the $f_3(x)$ states that the sample space does not contain nodules with radii belonging to this scope.

This paper presents a virtual experiment that proves the conclusion of the absence of particles with particular sizes. In order to do this, a simple computer program in the C++11 language has been written. Having such a program it was possible to generate sets of nodules with any imposed PDF_3 of their size and with ranges of particle sizes where they did not occur. The program also permitted creating random secant that pierced the nodules in order to get a set of chords. These chords have been employed to build histograms that approximated the functions $f_1(x)$. An analysis of the histograms showed that they have proportional dependences exactly in the same ranges in which the virtual sample spaces do not contain particles.

2. Virtual experiment

The form of the virtual sample space which has been used in the experiment is depicted in Fig. 1. In order to perform such an experiment, it was necessary to do a few things. The first step was a creation of a virtual volume of the shape of a cuboid. The size of the volume was $W \times D \times H$. Next, before the drawing of the nodules, it was necessary to impose a PDF_3 that described the particles' sizes. All generated nodules had to meet a few requirements. Their radii were ruled by the chosen PDF_3 and the location of their centres by a uniform real distribution. The nodules could not penetrate each other. The total particle count was a random variable. To provide this assumption the count of all particles was driven by an imposed value of ϕ_{max}. The parameter ϕ_{max} was a maximal volume fraction of the nodules which could not be exceeded.

Having the volume filled by the particles it was possible to insert a random cutting plane into the sample space. This plane split some encountered nodules producing marks of their surfaces. In the next step, a series of parallel secants has been placed on the cutting plane. These secants which intersected the marks produced sets of chords with random lengths.

The algorithm used in the program is presented in a general form as a flowchart in Fig. 2. Some of the computational steps have been labelled as Stage 1,..,8 in order to give more explanation in the text.

Stage 1: As the first step it is required to set the size of the sample volume and the value of ϕ_{max}. The parameter ϕ_{max} is fixed during the whole drawing process. Even though its constant value, the exact count of the generated particles is not possible to predict, because both the nodule sizes and their positions are random variables.

Stage 2: The probability density function of the nodule radii is selected at this stage. To generate random values of the radii, the standard C++11 function templates have been incorporated into the program. For example, for continuous uniform distribution of the nodule positions, the function that returns such values is named std::uniform_real_distribution<float>, and for normal distribution std::normal_distribution<float>. Other functions that can be included in the program are described in [9].

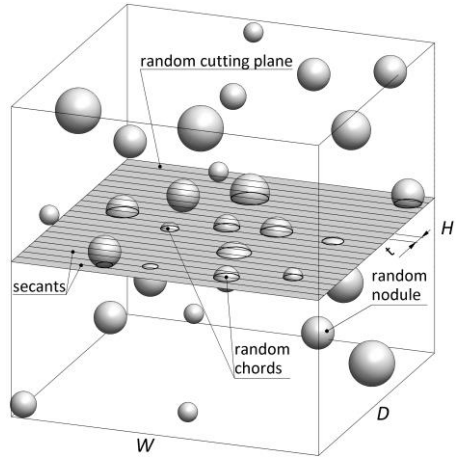

Fig. 1. A scheme of the virtual sample space with randomly generated nodules and chords

Stage 3: Drawing a random nodule radius and assigning its value to the float type. The value is generated according to the distribution selected at stage 2.

Stage 4: The position of the nodule centre in the sample space is ruled by the uniform real distribution. The range in which each coordinate is drawn is the following: [0, *W*], [0, *D*], [0, *H*] for the *x*, *y*, *z* coordinate, respectively.

It is important to divide the drawing process of the radius and the coordinates into two separate stages. Each volume of a new generated particle is checked whether it penetrates the volume of any previous one or not. If yes, a new set of random coordinates is drawn but the value of an old radius is kept. In case of drawing a new value of the radius too, the potential nodules with smaller radii find more likely an empty space for their location than the ones with larger sizes. This causes that the mean value of the radius of all generated particles is significantly lowered in comparison to the value imposed at stage 2.

Stage 5: Checking interpenetration between a currently created particle and the volume of all previous ones.

Stage 6: Each new particle has i_{max} times of attempts to locate itself somewhere in an empty space. If this value is exceeded, the drawing routine is ended and the program jumps to creating chords. This condition protects the program against looping an infinite number of times.

Stage 7: Checking the value of the current volume fraction of all nodules. If this value is less than the value of ϕ_{max}, the program continues generating new particles until the ϕ_{max} or i_{max} is reached.

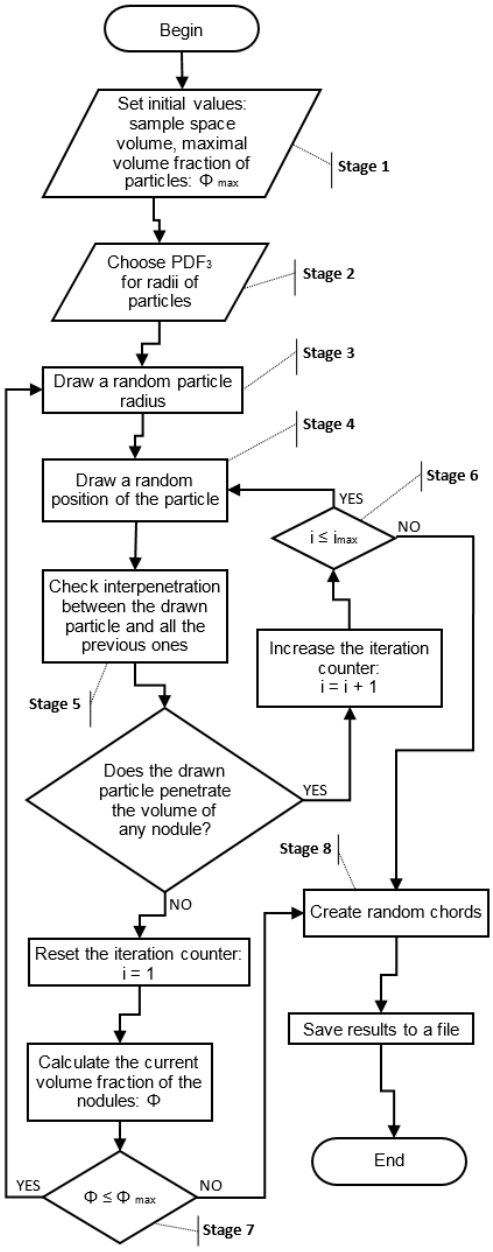

Fig. 2. Flowchart of the algorithm used to generate virtual spherical particles with imposed PDF_3 of the radii

Stage 8: When the drawing process is ended, the program produces random chords and saves their half-lengths to a file.

Some parameters of the virtual experiment, listed in Table 1, were the same for all imposed PDF_3. The denotation "ul" used as a unit means any unit of a length.

Table 1.
Values used in the virtual experiment

Description	Symbol	Value	Unit
sample space volume	$W \times D \times H$	1000×1000×100	ul
the maximal volume fraction of generated nodules	ϕ_{max}	0.15	–
the maximal number of attempts to locate a single particle	i_{max}	1000	–
scan step (the distance between parallel secants)	t	2	ul

3. Results

Four series of calculations have been performed for imposed distributions of 3D nodules.

Parameters set in the program and obtained results are listed in Table 2. The values written in the normal font have been imposed in the program, whereas the outcomes in bold are random results obtained from the program.

Table 2.
Parameters used in calculations and obtained results

Description	Symbol	Value	Unit
Constant radius			
Nodule radius	R_3	50.00	ul
Total count of drawn nodules	N_r	**2864**	–
Total count of created chords	N_c	**110807**	–
Continuous uniform distribution			
Lower bound	$R_{3,l}$	30.00	ul
Upper bound	$R_{3,u}$	60.00	ul
Total count of drawn nodules	N_r	**3546**	–
Total count of created chords	N_c	**108228**	–
Bimodal continuous uniform distribution			
Left lower bound	$R_{3,ll}$	20.00	ul
Left upper bound	$R_{3,lu}$	30.00	ul
Right lower bound	$R_{3,rl}$	50.00	ul
Right upper bound	$R_{3,ru}$	60.00	ul
Total count of drawn nodules	N_r	**3777**	–
Total count of created chords	N_c	**104881**	–
Bimodal normal distribution			
Left mean	μ_l	30.00	ul
Left standard deviation	σ_l	1,50	ul
Right mean	μ_r	60.00	ul
Right standard deviation	σ_r	3.00	ul
Total count of drawn nodules	N_r	**2969**	–
Total count of created chords	N_c	**94533**	–
Left lower bound	$R_{3,ll}$	**25.41**	ul
Left upper bound	$R_{3,lu}$	**35.53**	ul
Right lower bound	$R_{3,rl}$	**50.49**	ul
Right upper bound	$R_{3,ru}$	**69.41**	ul

First calculations have been performed for a sample volume with nodules having a constant radius. The value of the radius was

equal to 50 ul. After creating random chords, the PDF_1 histogram has been prepared in the form of which is presented in Fig. 3. Equation (2) states that the histogram's values should have a proportional dependency in the range from 0 to the minimal nodule radius R_3. This statement results from the fact that the sample volume did not contain nodules with a radius lesser than the value of R_3 = 50 ul. The function CDF_3 in Eq. (2) takes zero in this whole range. As it is seen, all the values (except the last one) fit well to the regression line. The coefficient of determination R^2 is close to 1. Equation (1) also states that this line should pass through the origin point. This means that the constant term in the regression equation must have the value of 0. The obtained value (0.0009) is practically equal to 0.

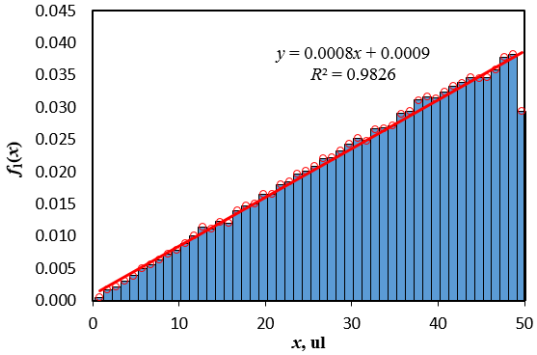

Fig. 3. The PDF_1 histogram obtained from the sample space with nodules having a constant radius. The interval width: 1 ul

The second set of generated particles have been created for a continuous uniform real distribution. The range in which the nodule radii have been drawn was from $R_{3,l}$ to $R_{3,u}$ ul (see the value in Table 1). The histogram that approximates the PDF_1 of the half-chord lengths is depicted in Fig. 4a. The red thick line presents a linear regression in the range of x from 0 to $R_{3,l}$ ul in which the nodules had not been produced (Fig. 4b). As it is seen the line fits very well to the histogram's values – the coefficient of determination R^2 is close to 1. The constant term is also very close to its theoretical value of 0.

Two afore presented histograms in Figs. 3 and 4 show that the values have the proportional dependency in the range from 0 to a minimal value of the radius. Equation (2) also states that this dependency should appear in every range where the particle radii do not occur. In such ranges, the cumulative distribution function (the $F_3(x)$ term) has to have a constant value, which also makes the function $f_1(x)$ proportional. In order to check this property next series of random nodules has been generated, this time for a bimodal continuous uniform real distribution. The histograms of the half-chord lengths and the nodule radii are shown in Fig. 5. The sample space contained two separate sets of particles. The first set, named left, has been created in the range of the radii from $R_{3,ll}$ to $R_{3,lu}$ ul, in turn, the second one, named right, in the range from $R_{3,rl}$ to $R_{3,ru}$ ul. Two regression lines in Fig. 5a fit very well to the histogram's values where the proportional dependences occur. Both coefficients of determination R^2_l and R^2_r are close to 1. Similarly, as it was in the case of the results presented in Figs. 3 and 4a, the constant terms are also close to 0. The outcomes obtained for the bimodal continuous uniform real distribution show clearly that the proportional dependency of the PDF_1 occurs also in the range between the left and right sets which are depicted in Fig. 5b.

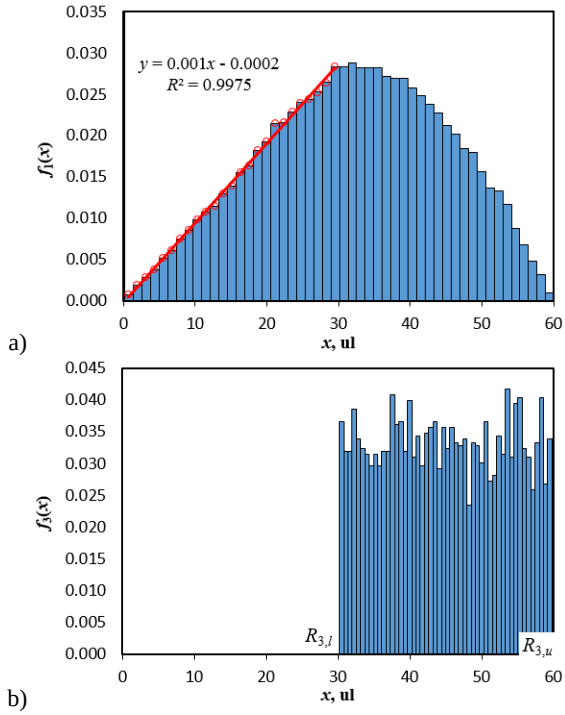

Fig. 4. Histograms created for the sample space ruled by the continuous uniform distribution: a) the PDF_1; the interval width: 1.2 ul; b) the real PDF_3; the interval width: 0.6 ul

The last set of random chords has been created on the basis of the sample space containing nodules with radii ruled by a bimodal normal distribution. The parameters such as the mean values and the standard deviations for this distribution are listed in Table 2. Because the normal distribution does not have strict lower and upper bounds of the nodule radii, it was necessary to find manually the scopes in which the nodules had not been created. The lower and upper bounds for the left and right sets seen in Fig. 6b are presented in Table 2. Having these values it was possible to add linear regressions in the scopes where the particles did not occur. As it is seen in Fig. 6a the left line fits well to the proportional scope of the PDF_1 histogram. The R^2_l coefficient is also close to 1 and the constant term close to 0. However, the right regression deviates more from the proportionality than the left one. What is more, the scope of the right linear regression is not as clearly seen as in the previous cases. Probably, this situation may deteriorate if the gap between the left and right sets will be narrower.

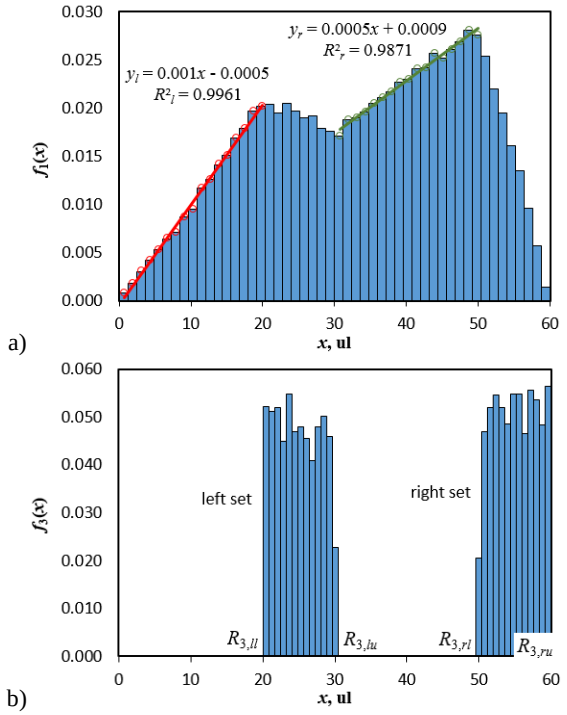

Fig. 5. Histograms created for the sample space ruled by the bimodal continuous uniform distribution: a) the PDF_1; the interval width: 1.2 ul; b) the real PDF_3; the interval width: 0.8 ul

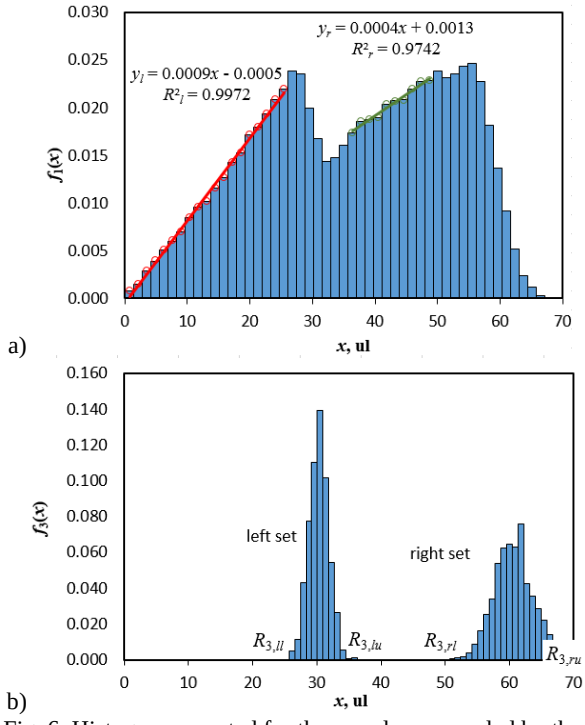

Fig. 6. Histograms created for the sample space ruled by the bimodal normal distribution: a) the PDF_1; the interval width: 1.37 ul; b) the real PDF_3; the interval width: 0.88 ul

4. Result analysis and conclusions

The presented histograms of the PDF_1 and the linear regressions prove that if a sample space does not contain particles with particular sizes, the function $f_1(x)$ is proportional in this range. However, it should be emphasized that the analysis of the histograms was facilitated because the PDF_3 distributions of the nodule radii were known (they have been imposed in the virtual experiment). This allowed finding accurately the scopes where the nodules did not occur. In practice, such information is not accessible. The form of the real PDF_3 is mapped e.g. by using Eq. (1) on the basis of random chords. But the chord method produces big noise on the mapped PDF_3 histograms in the range of small chords. This fact has been presented in [10]. For this reason, the mapped PDF_3 is useless for the accurate determination of the ranges in which the linear regressions can be applied.

For all analysed distributions of the nodule radii, the proportional dependency is clearly seen on the PDF_1 histograms in the range from 0 to the smallest particle radius. All the red regression lines fit very well to the values and their coefficients (R^2 and the constant terms) are close to 1 and 0, respectively. In the case of the bimodal distributions, in the gap between the left and right sets, the proportional dependency is also visible. But for the bimodal normal distribution, the proportional range (the green line in Fig. 6b) deviates more from the theoretical behaviour than the previous ones.

Obtaining in real measurements a histogram having a character like the one in Fig. 3 may provide two important things. The first one, which has been mentioned in this paper, is the absence of nodules with particular radii. The second one is the fact that we can state with a large probability that all particles have the same size.

The presented method for a finding of the ranges of the nodule absence requires further improvement. Some mathematical criteria must be elaborated which will permit unequivocally determining the ranges where the linear regressions can be used and where not.

Despite the fact that all calculations have been performed virtually, the method may have practical application in foundry engineering. The authors of the paper published in [11] showed that eutectic grains in grey cast iron can nucleate in some cases in two separate stages. To prove this, the researchers executed computer calculations that were supported by experiments. If a similar phenomenon occurred in the case of the spheroidal graphite nucleation, it would have not been possible to detect it by a simple analysis of nodules' cross-sections on a metallographic specimen. It is not possible to state how big the intersected nodules were having only the radii of their sections. The presented analysis of the proportional ranges on histograms obtained on the basis of such nodular cast iron would allow us to detect a similar proportional scope like in Figs. 5a or 6a (marked by the green lines). This would suggest that graphite nucleation has been divided into two stages.

Acknowledgement

The research was financially subsided by the Department of Engineering of Cast Alloys and Composites at AGH University of Science and Technology, Faculty of Foundry Engineering.

References

[1] Gurgul, D., Burbelko, A. & Wiktor T. (2021). Derivation of equation for a size distribution of spherical particles in non-transparent materials. *Journal of Casting & Materials Engineering*. 5(4), 53-60.

[2] Wicksell, S.D. (1925). The corpuscle problem: mathematical study of a biometric problem. *Biometric.* 17 (1/2), 84-89.

[3] Sheil, E. (1935). Statistische gefügeuntersuchungen I. *Zeitschrift für Metallkunde*. 27 (9), 199-208.

[4] Schwartz, H.A. (1934). The metallographic determination of the sze distribution of temper carbon nodules. *Metals and Alloys.* 5, 139-140.

[5] Saltykov, S.A. (1967). The determination of the size distribution of particles in an opaque material from the measurement of the size distribution of their section. in the second international congress for stereology, Chicago, 8-13 April 1967. Berlin–Heidelberg–New York, Springer Ver-lag.

[6] Cahn, J.W. & Fulmann, R.L. (1956) On the use of lineal analysis for obtaining particle size distributions in opaque samples. Transactions, American Institute of Mining, *Metallurgical and Petroleum Engineers*. 206, 177-187.

[7] Lord, G.W. & Willis, T.F. (1951). Calculation of air bubble size distribution from results of a rosiwal traverse of aerated concrete. *ASTM Bulletin*. 177, 177-187.

[8] Spektor, A.G. (1950). Analysis of distribution of spherical particles in non-transparent structures. *Zavodsk. Lab*. 16, 173-177.

[9] https://www.cplusplus.com (date of access 06.06.2021).

[10] Burbelko, A., Gurgul, D., Guzik, E. & Kapturkiewicz, W. (2018). Stereological analysis of the statistical distribution of the size of graphite nodules in DI. *Materials Science Forum.* 925, 98-103.

[11] Fras, E., Burbelko, A.A. & Lopez, H.F. (1996). Secondary nucleation of eutectic graphite grains. *Transactions of the American Foundrymen Society*. 104, 1-4.